Journal of Materials Chemistry C

Accepted Manuscript

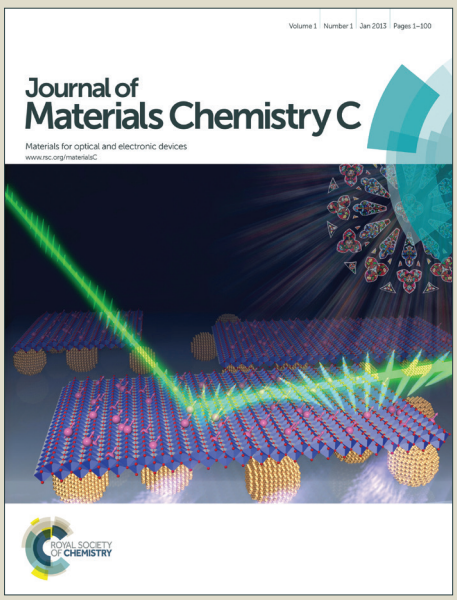

ROYAL SOCIETY OF CHEMISTRY

www.rsc.org/materialsC

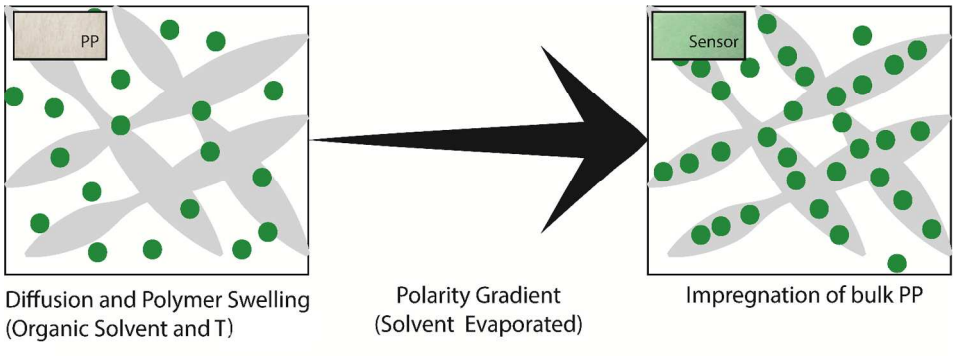

468x164mm (96 x 96 DPI)

Journal of Materials Chemistry

RSCPublishing

ARTICLE

Phosphorescent O_2 sensors based on polyolefin fabric materials

Cite this: DOI: 10.1039/x0xx00000x

Caroline A. Kelly[a♦], Claudio Toncelli[b♦], Joe Kerry[b], Dmitri B. Papkovsky*[b]

Received 00th January 2012,
Accepted 00th January 2012

DOI: 10.1039/x0xx00000x

www.rsc.org/

New phosphorescent oxygen sensors based on non-woven polypropylene membranes with grafted and ungrafted monofibres were created and evaluated. The two-component materials were fabricated by simple swelling of the polymeric fabric and partitioning of the phosphorescent dye molecules in appropriate solvent system. The resulting sensors exhibited high brightness, optimal lifetime signals (22-30 μs at 21 kPa and 50-60 μs at 0 kPa O_2), linear Stern-Volmer plots, temperature dependence and low cross-sensitivity to humidity. Compared to state-of the-art O_2 sensors (PS coating on the microporous support), the new PP-based sensors performed well, showing good wettability and fast response time in liquid (5 min for grafted and 7 min for ungrafted PP vs 32 min for the reference), mechanical stability without any additional support. Microscopic analysis of the PP fabric sensors by PLIM confirmed homogenous dispersion of the dye throughout the membrane and uniformity of O_2 sensing properties.

1. Introduction

Optical detection of molecular oxygen (O_2) is important for biological research[1], clinical and medical applications[2], aerodynamics,[3] process control in the chemical industry,[4] environmental monitoring,[5] plant science,[6] pharmaceutical[7] and food packaging applications.[8] Ideally, a sensor should be stable, robust, easy-to-use and not prone to electrical interferences nor consume O_2.[9, 10] Solid-state O_2 sensors based on quenching of long-decay fluorescent and phosphorescent dyes satisfy many of these criteria. They usually consist of an indicator dye encapsulated within an O_2 permeable polymer matrix.[11] The polymer matrix, particularly its dye compatibility, oxygen permeability, wettability and chemical resistance, mechanical properties and processability, greatly influence sensor performance.[12] Common plastics with high and moderate O_2 permeability, such as polystyrene, polydimethylsiloxane, fluorinated polymers and co-polymers, plasticized polyvinylchloride have been extensively used as encapsulation matrices for quenched-phosphorescence O_2 sensors.[9] Such O_2 sensors are usually produced by solution based processes, whereby the polymer is dried from a cocktail in organic solvent,[13] or formed by polymerization or curing of liquid precursors (silicones, ormosils, sol-gels[14]). Other methods of dye incorporation include adsorption,[15] covalent binding,[16] solvent crazing[17] and polymer swelling methods.[10]

The thin film nature of the O_2 sensors, which avoids the creation of significant barriers for O_2 diffusion, usually requires an additional support material being incorporated into the sensor structure. The support improves mechanical properties of the sensor material, facilitates its handling and optical measurements.[18] The main types of support materials are planar gas-impermeable solid substrates, such as glass or PMMA slide, polyester film Mylar[13], or flexible gas-permeable microporous membranes.[19] Microporous supports having a sponge-like structure, light-scattering properties and significant thickness provide enhanced optical signals, good mechanical properties and reasonably fast response times in the gas phase. However, hydrophobicity of the polymeric coating often leads to poor wettability of the sensor and slow response in aqueous samples.

Although successful in many applications, existing sensor materials, fabrication processes and polymeric matrices are not very compatible with large-scale applications such as packaging, which involve mass manufactured materials (e.g. gas-barrier and heat-sealable films and laminates) and processes (e.g. modified atmosphere packaging, MAP). For such applications characterized by low profit margins and large scale manufacturing output conventional sensor technologies appear to be too complex, inflexible and expensive. Each sensor should cost less than 1c per cm^2,[2,20], and exhibit reproducible, stable and calibration-free operation. Such working specifications necessitate development of new types of sensor materials, as well as their fabrication and integration technologies.

Polypropylene (PP) and polyethylene (PE) are the most common packaging materials which total over half of the amount of polymers produced globally.[21] Mechanical and gas-permeability properties of PP and PE are very capable of O_2 sensing,[22] however their insolubility in common organic solvents and incompatibility with many O_2 sensitive dyes, make difficult their use in fabrication of O_2 sensors by traditional means.

Nonetheless, PP and PE have been used to produce O_2 sensors by solvent-crazing[22] and hot polymer extrusion[23] processes, showing good potential for packaging applications. Recently, non-woven polyolefin materials have been developed for use in textiles, sport and medical wear, membranes, carpets, filtration systems[12] and

charge separators in Li-ion batteries.[24] These materials are now produced on large industrial scale, have suitable chemical, mechanical and thermal stability, gas permeability, uniformity and thicknesses between 20-150 microns.[12, 25] They also possess micro-porosity, light-scattering properties, large surface area and affordable cost.[24-27]

Unmodified polyolefine based non-wovens are generally hydrophobic. They are used in solvent based applications (e.g. filtration), but wettability in aqueous samples can be problematic. This can be altered by the grafting of hydrophilic chemical groups or polymeric chains to the surface of monofibres[12, 28, 29], e.g. by plasma treatment, UV and gamma radiation, ozone and $(NH_4)_2S_2O_8$[12]. Such materials are more hydrophilic than ungrafted precursor and show higher uptake of polar solvents, reduced membrane fouling and reduced permeability.[12, 24, 26]

In this study, we evaluated several non-woven materials based on grafted and ungrafted PP as a matrix for fabrication of O_2 sensors. The small size of their monofibres, high chemical and mechanical stability and microporous structure enable their straightforward use for fabrication of optical O_2 sensors, without any additional support. We applied simple impregnation by polymer swelling and dye partitioning in organic solvent system, which has been used with polymeric micro and nanoparticles[30], but not with non-woven polyolefine materials. We optimised the impregnation method and produced simple two-component sensors based on the polymeric matrix and phosphorescent dye PtBP, and showed that they display usable O_2 sensing characteristics and analytical performance.

2. Experimental

2.1 Materials

The non-woven spun bond PP grafted with acrylic chains (Type 700/70, thickness 130µm ± 20 µm, fibre size 8-12 micron, weight – 55 g/m2, mean pore size 17 µm) and the ungrafted PP (Type FS2192i, thickness 80µm ± 20 µm, mean pore size 17 µm, fibre size 8-12 micron) were purchased from Freudenberg, UK. Platinum (II)-benzoporphyrin dye (PtBP) was from Luxcel Biosciences (Cork, Ireland). The toluene (≥ 99.3%) and tetrahydrofuran (HPLC grade) were from Sigma-Aldrich, and N_2 and O_2 gases (99.999% purity) - from Irish Oxygen (Ireland).

For the impregnation, a solution of PtBP dye in 70:30 THF/H_2O (0.03 mg/ml) was prepared and 8 mL aliquots were placed in disposable 15 mL plastic vials (Sarstedt). Strips of PP material (24x12 mm) cut out from the sheets were inserted in each vial (one per vial immersed in solution). The vials were then capped, placed in an oven set at 65˚C and incubated for 1 h. After this sensor strips were extracted from the vials, rinsed with water and dried in air for 18 h. Subsequently they were incubated in dry oven at 70˚C for 16 h. Optionally, after the incubation step; the solvent was evaporated by incubating the opened vial at 40˚C for 16 h. In this case the membrane remained submerged in water.

The amount of dye encapsulated in each sensor was estimated by extracting the dye from the sensor with toluene (1 mL in 1.5 mL vials, 24h incubation at 50˚C), followed by absorbance measurement of the supernatant. A calibration curve was generated by serial dilutions of dye stock (0.1 mg/mL in toluene).

2.2. Spectroscopic characterization of sensors

For screening and optimization experiments phosphorescence intensity and lifetime signals were recorded with a handheld instrument Optech™ (Mocon, Minneapolis, USA) using the sensors placed in a clear 20 mL polystyrene vial (Sarstedt, Ireland). Each sensor strip was measured five times in different locations and average values and S.D. were calculated.

Dry and humid gas calibrations of the sensors were performed with a Firesting™ instrument (PyroSciences GmbH, Germany) which operates with a 1 mm plastic fibre probe under standard manufacturer's settings. The probe was brought in contact with the sensor, phase shift readings were measured and converted into lifetime values as follows: $\tau = \frac{\tan(\theta)}{(2 \cdot \pi \cdot \vartheta)}$, where τ is the lifetime (µsec), θ - phase shift (in radians), and ϑ - modulation frequency of excitation (4.0 kHz).

For sensor calibration standard O_2/N_2 gas mixtures (0-100 kPa O_2) produced by a precision gas mixer (LN Industries SA, Switzerland) were pumped through a flow cell with a glass window through which an O_2 sensor was interrogated with the Firesting™ instrument. The flow cell was submerged in a circulating water bath (Julabo) keeping the window and probe above water level to equilibrate the gas to the correct temperature.

2.3 Microscopic measurements

Wide-field optical imaging was performed on an inverted microscope Axiovert 200 equipped with Plan Neofluar 40x/1.3 oil immersion objective (Carl Zeiss), pulsed excitation module (590 nm LED), gated CCD camera (LaVision Biotech), excitation 595/40 nm and emission 780/60 nm filter cube, and incubation chamber with O_2 and temperature control (PeCon). Frame time in fluorescence and differential interference contrast (DIC) imaging was 100-150 ms. Phosphorescence lifetime imaging (PLIM) settings (Delay T, snapshot mode) at 21 kPa O_2 were: pulse width 10 µs, repetition time 170 µs, gate time 10 µs, delay time 0-100 µs (11 images); frame time 100 ms, no binning. At 1 kPa O_2 the settings were: pulse width 10 µs, repetition time 190 µs, gate time 20 µs, delay time 0-120 µs (11 images); frame time 100 ms, no binning.

3. Results and Discussion

3.1. Sensor design and general considerations

The polymeric substrates selected for O_2 sensor development consist of a large number of small PP monofibres bound together in planar flexible sheets.[25] These structures possess high surface area, good mechanical and light-scattering properties and the option of modification of the surface of monofibres by grafting. The grafted PP matrix provides a hydrophilic and wettable surface and hydrophobic bulk material

(unmodified PP). These features of the microporous polyolefin fabric are very beneficial for optochemical sensing applications.

Table 1. Effects of the main process parameters on sensor intensity (I) and lifetime (τ) signals in N_2 (0 kPa O_2) and air (21kPa O_2).

Parameter	Variation	Material	τ_0	τ_{21}	I_0	I_{21}
Solvent	Toluene	Grafted[a]	48.21 ± 1.07	30.39 ± 0.10	2550 ± 610	1151 ± 255
	THF (100%)	Grafted	49.29 ± 0.67	33.78 ± 0.13	5556 ± 485	2709 ± 215
	THF (80%)	Grafted	51.03 ± 0.30	33.41 ± 0.06	5805 ± 626	2757 ± 317
	THF (70%)	Grafted	50.21 ± 0.52	33.68 ± 0.04	14161 ± 1314	6796 ± 573
Dye conc.	0.025 mg/mL	Grafted	50.77 ± 0.01	29.53 ± 0.02	10752 ±758	4446 ± 272
	0.035 mg/mL	Grafted	49.54 ± 1.85	32.55 ± 0.24	15778 ± 2316	7340 ±1059
Annealing Status	Annealed	Grafted	50.80 ± 0.34	33.75 ± 0.09	2527 ± 349	1404 ± 221
	Not Annealed	Grafted	49.20 ± 0.93	32.82 ± 0.16	3767 ± 846	1771 ± 298
Drying regime	Solvent evaporation	Grafted	51.25 ± 0.48	32.25 ± 0.05	5438 ± 696	2274 ± 347
	Air dried	Grafted	50.80 ± 0.34	33.75 ± 0.09	2527 ± 349	1404 ± 221
Optimized Sample		**Grafted**	**50.77 ± 0.01**	**29.53 ± 0.02**	**9896.71 ± 467.50**	**4271.80 ± 239.35**
		Ungrafted	**57.32 ± 0.09**	**22.45 ± 0.07**	**7539.00 ± 276.05**	**3485.86 ± 86.65**

[a]Initial optimization was performed on the grafted PP membrane

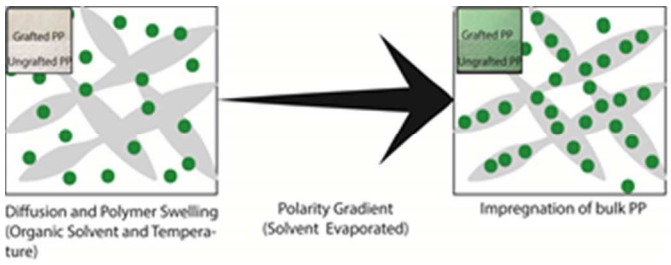

Fig. 1. Proposed impregnation of PP fabric membrane by swelling in dye solution.

In particular, simple impregnation by swelling the polymer in organic solvent contained hydrophobic dye can be used - an approach commonly used with suspensions of polymeric micro particles.[30] Such materials do not require additional support and have a simple binary composition with only the dye and encapsulation matrix.

Using this strategy, we optimised the production of phosphorescent O_2 sensors based on non-woven PP substrates and PtBP dye and studied the effects of its main parameters. According to the manufacturer, spun bond materials are made from pure propylene with average fibre diameters of 8-12 µm.[31] The non-woven web consists of continuous fibres that are produced by melt extrusion. Fibre bonding is achieved either by pin bonds or mild thermal bonding. Grafted further enhances the properties of this material. The material was grafted with acrylic acid in a two-step process. Initially, free radicals were created on the surface of the polymer using UV radiation which combines with hydrophilic vinyl monomer units to produce a growing chain. This grafting maximises wettability and the wicking characteristics and prevents degradation of the base layer.

To facilitate incorporation of hydrophobic dye molecules in hydrophobic bulk polymer (PP), we applied a gradient of polarity during the impregnation, whereby the low polarity solvent was gradually removed by evaporation from the dyeing solution (a mixture with relatively low water content which dissolves the dye and swells the polymer).[32] This forced the dye molecules to partition favourably between the hydrophobic bulk polymer and hydrophilic aqueous solution or grafted phase. In addition, the raised polarity of the solution also causes the polymer to de-swell and trap the dye molecules. Elevated temperatures (below solvent boiling) were also used to speed up the diffusion and re-equilibration processes in the system. The dye encapsulation process is shown on Fig. 1.

3.2. Optimisation of sensor fabrication and initial screening

Systematic optimisation of the process was carried out in a one-variable-at-a-time fashion, aiming to achieve high intensity, stable lifetime signals from individual sensors and good reproducibility of optical readings between the sensors. The results are collated in Table 1.

The solvent is paramount for the penetration of the dye into the polymer matrix. In order to be effective, the solvent system must be compatible with the dye and not degrade the polymer. As polypropylene is highly chemical resistant, there are very few non-suitable solvents. The hydrophobic dye is soluble in non-polar solvents such as THF, ethyl acetate, butanone and toluene, of which THF was the most efficient showing highest phosphorescent intensity and lifetime signals in nitrogen. In the other solvents there was evidence of partial aggregation and quenching of the dye after impregnation.

Journal of Materials Chemistry RSCPublishing

ARTICLE

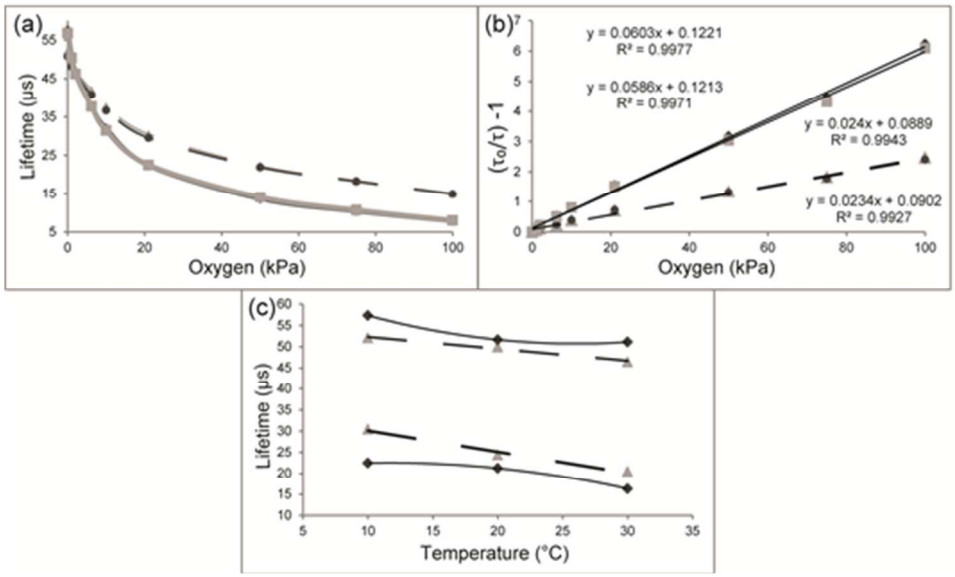

Fig. 2 (a) O_2 calibrations of grafted PP (dashed line) sensors in dry gas (▲) and humid gas (●) and ungrafted PP (solid line) in dry gas (♦) and humid gas (■) presented in lifetime scale. (b) Corresponding Stern-Volmer plots. (c) Temperature dependence of grafted and ungrafted PP sensors at 21 kPa and 0 kPa in dry gas.

We also found that with the grafted PP, pure solvents were not providing adequate intensity signals perhaps due to a lack of compatibility between the solvent, dye and polymer, while their mixtures with high polarity solvents such as water worked better. The best intensity signals were observed in the 70:30 THF:H_2O, particularly when the solvent was evaporated off after the incubation leaving the aqueous medium to surround the sensor sheet. Optimal dye concentration was 0.025 mg/mL.

The incubation time was varied between 1 h, 2 h and 3 h. Longer incubation times did not yield higher lifetime or intensity signals, therefore it was set at 1 hr. Likewise the incubation temperature was varied from 60˚C to 70 ˚C yielding the highest lifetime and intensity signals at 65 ˚C.

Slow solvent evaporation of the liquid-immersed samples at 40˚C, allows the dye more time to penetrate into the membrane. This in turn increases the concentration of the dye within the PP membrane raising its intensity signal by approximately 116%.

Table 2 Response Times in Liquid @ 10C

Sample	21% to 10% O_2	10% to 21% O_2	Wetting Time
Grafted PP	5 min 16 sec	5 min 09 sec	2 min 31 sec
Ungrafted PP	7 min 21 sec	7 min 01 sec	2 min 00 sec
PS coating on porous support	31 min 55 sec	27 min 53 sec	> 30 min

Annealing of polymeric sensors often improves their performance due to elimination of internal stresses and defects in the polymer[33]. Indeed, Table 1 shows that annealing increased lifetime signals in nitrogen and air, reduced their variability (S.D.) resulting in better uniformity of sensor structures. Therefore, the annealing step was included in sensor fabrication.

For comparison, we also prepared O_2 sensors based on the ungrafted PP. Different ratios of THF and water were also tested and the optimum was found at 50:50 ratio. The solution becomes increasingly polar as the THF is volatised into gaseous form during incubation. As a result, the hydrophobic dye molecules transfer from the polar solution into the hydrophobic membrane. Although the lifetime and intensity signals for the ungrafted PP favoured the 0.035 mg/mL, the difference was too small to justify the higher dye concentration and 0.025 mg/ml was chosen as optimal. High signals obtained from the ungrafted PP membrane after the incubation and simple drying, made the solvent evaporation step unnecessary. This feature was attributed to the higher hydrophobicity and/or different structure of the ungrafted PP membrane, which facilitated higher diffusion of the dye within the membrane.

Analysis of the dye extracts from each sensor resulted in estimated amounts of 0.57 µg in the grafted and 0.39 µg in the ungrafted PP sensors, respectively. Batch to batch variability was assessed by looking at mean lifetime values and relative standard deviations (RSD). For the six samples of grafted PP sensor the RSD was found to be 2.90% at 21 kPa and 0.94% in 0 kPa. In

comparison the RSD of the ungrafted PP sensor was found to be 2.19% in air and 2.16% in nitrogen for four samples.

3.3. Detailed characterisation of optimised sensors

Detailed characterisation included full O_2 calibrations (0-100 kPa) performed both in dry and humid (passed through a humidifier) gas and temperatures 10, 20 and 30°C. This covers the mean temperature and O_2 ranges that food and pharmaceutical products are stored at and hence the O_2 sensors should be used. Both grafted and ungrafted PP sensors were measured; the results are shown in Fig. 2.

For the grafted PP in dry gas conditions at 10°C, going from 0 kPa oxygen to 100 kPa sensor lifetime signal decreased from 50.77 +/- 0.01 µs to 14.90 +/- 0.01 µs. In humid gas, the changes in sensor lifetime signal at 0-100 kPa O_2 were within experimental error. For the ungrafted PP sensor in the gas phase at 10°C the lifetime changed from 57.32 +/- 0.09 µs to 7.93 +/- 0.01 µs when going from 0 kPa to 100 kPa.

The Stern-Volmer plots inform on sensor homogeneity and the quenching constant[34]. Higher Stern-Volmer constant reflects higher sensitivity of the sensor to O_2 [35]. The ungrafted PP sensor was approximately twice more sensitive to O_2 than grafted. Since bulk polymer is the same (PP), the difference is probably due to their fabrication methods (fibre bonding, chemical and mechanical treatment). The ungrafted PP is significantly thinner. The limits of detection (LOD) which were calculated as 3*S.D. were 0.09 kPa and 0.27 kPa at zero and 21 kPa O_2, respectively.

Dynamic quenching is strongly influenced by the temperature[36, 37]:

$$\frac{1}{\tau} = k^0{}_f + A_{nr}.e^{\frac{-\Delta E_{nr}}{RT}} + A_q{}^0.e^{\frac{-\Delta E_q}{RT}}$$

where $k^0{}_f$ - kinetic constant of the fluorescent decay, A_{nr} - pre-exponential of non-radiative process, $A_q{}^0$- pre-exponential of the quenching process ΔE - activation energies of the non-radiative and quenching process respectively, R - gas constant, T - absolute temperature. The negative slopes indicate that luminophore lifetime is decreasing as temperature increases. For a narrow T-range, a linear dependence of lifetime is desirable, as it allows T-compensation by simple algorithms. For the grafted PP the T-dependence appears to be linear, while in the ungrafted PP the plots display pronounced curvature (polynomial fitting).

Linear Stern Volmer plots are desired for solid-state sensors, as this allows simple calibrations (two-point or even one). This depends on micro-heterogeneity of the polymer and uniformity of dye dispersion in it [38]. We observed linear Stern-Volmer plots for both membranes.

Hydrophobic polymeric sensor coatings on microporous support materials often lead to poor wettability, formation of micro-bubbles within sensor material and slow response to changes in O_2 concentration in aqueous samples[18]. However, the PP sensors showed fast response both in the gas and liquid phase, unlike the conventional microporous sensors which responded 4-5 times slower. The grafted ~~ungrafted~~ membrane was slightly faster than ungrafted one (due to higher hydrophilicity), and the responses were fully reversible. The results are shown in Table 2 (at 10˚C).

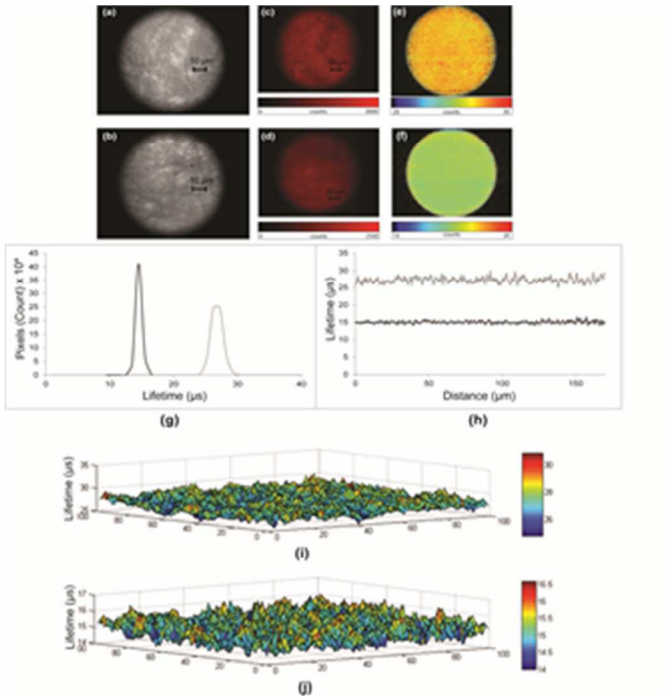

Fig. 3. Wide-field microscopy images of grafted and ungrafted PP sensors: (a, b) bright field images of grafted and ungrafted PP ~~(a, b)~~; (c, d) phosphorescence intensity images of grafted and ungrafted sensors respectively ~~(c, d)~~; (e, f) PLIM images grafted and ungrafted sensors ~~(e,f)~~, (g) histograms ~~(g)~~ & (h) line profiles of grafted and ungrafted PP ~~(h)~~ (light grey – grafted, dark grey - ungrafted), (i, j) 3D surface graphs ~~(i,j)~~ of lifetimes of grafted and ungrafted sensors . Sample area analysed: 100 x 100 pixels, 11536.21 µm^2. Measured at room temperature, 21 kPa, 40X magnification.

3.4. Microscopic Analysis

Wide-field optical microscopy and FLIM were used to analyse the fine structure and uniformity of dye distribution in the sensing membranes. As the films were relatively thick and non-transparent, it was only possible to focus on one section at a time. The bright field images in Fig. 3a, b depict the top layer of each membrane. As can be seen, the ungrafted PP exhibits narrower fibres than the grafted PP, again probably due to different methods used in their manufacture.

Phosphorescence images were obtained under high (21 kPa) and low (1 kPa) O_2. The intensity images acquired in air (Fig. 3c,d) correlate with the features seen in the bright field images, with the brighter regions corresponding to areas of higher fibre density (more dye being entrapped between the more closely knit fibres in these areas). The phosphorescent lifetime images showed a higher homogeneity than intensity images, with the grafted PP showing a wider dispersion of lifetime than ungrafted PP ranging across the field of view 27.25 ± 0.77 µs and 15.00 ± 0.34 µs, respectively (Fig. 3e,f). These observations are supported by the line profiles and histograms (Fig. 3g,h) generated from the lifetime images on which the distribution of pixel intensities for the selected sections of the sensor can be seen[39]. The 3-D shaded surface graphs (Fig. 3i, j) show

that the spread of lifetimes is relatively uniform in the sensor membranes.

Overall, as the distribution of phosphorescence lifetime in air for the ungrafted PP is Gaussian in nature and relatively narrow, we can conclude that the luminophore molecules are dispersed quite uniformly and have homogeneous micro-environment throughout the sensor. This is concurrent with the linear Stern-Volmer plots for O_2 calibrations. The grafted PP sensors, despite the lower quenching of the dye and higher intensity signals, showed broader distribution and asymmetry of the lifetime values.

3.5. Conclusions

Sensors from the two types of polypropylene fabric material were created which show good wettability, high signals and stable calibrations in both dry and humid mediums. As the grafted PP shows lower sensitivity, it could be applied to monitoring of higher O_2 concentrations (0-100 kPa). The ungrafted PP is better suited for monitoring of low O2 levels (0-21 kPa). Further studies will be performed on these sensors to access their scalability, performance and safety in food packaging applications.

Acknowledgement

Financial support of this work by the Irish Department of Agriculture, Food and Marine, grant DAFM 11/F/015, is gratefully acknowledged. Authors thank Dr. R. Dmitriev for the help in imaging experiments.

Notes and references

[a] *Department of Biochemistry, University College Cork, Cavanagh Pharmacy Building, College Road, Cork, Ireland. Fax: +353-21-490-1698; Tel: +353-21-490-1698; E-mail: d.papkovsky@ucc.ie*
[b] *Department of Food Science and Nutrition, University College Cork, Cavanagh Pharmacy Building, College Road, Cork, Ireland*
♦ *- these authors contributed equally to this work*

1. D. B. Papkovsky and R. I. Dmitriev, *Chemical Society Reviews*, 2013.
2. D.F. Lee, H.P. Kuo, M. Liu, C.K. Chou, W. Xia, Y. Du, J. Shen, C.T. Chen, L. Huo, M.C. Hsu, C.W. Li, Q. Ding, T.L. Liao, C.C. Lai, A.-C. Lin, Y.H. Chang, S.F. Tsai, L.Y. Li and M.C. Hung, *Molecular Cell*, 2009, **36**, 131-140.
3. T. Liu, M. Guille and J. P. Sullivan, *AIAA Journal*, 2001, **39**, 103-112.
4. T. Hyakutake, H. Taguchi, H. Sakaue and H. Nishide, *Polymers for Advanced Technologies*, 2008, **19**, 1262-1269.
5. M. Quaranta, S. M. Borisov and I. Klimant, *Bioanalytical reviews*, 2012, **4**, 115-157.
6. C. Ast, E. Schmälzlin, H.-G. Löhmannsröben and J. T. van Dongen, *Sensors*, 2012, **12**, 7015-7032.
7. T. Lenarczuk, S. Głąb and R. Koncki, *Journal of Pharmaceutical and Biomedical Analysis*, 2001, **26**, 163-169.
8. A. Hempel, M. Sullivan, D. Papkovsky and J. Kerry, *Foods*, 2013, **2**, 213-224.
9. Y. Amao, *Microchim. Acta*, 2003, **143**, 1-12.
10. A. Mills, *Platinum Metals Rev*, 1997, **41**, 115-127.
11. S. M. Borisov, T. Mayr and I. Klimant, *Analytical chemistry*, 2008, **80**, 573-582.
12. L.S. Wan, Z.M. Liu and Z.K. Xu, *Soft Matter*, 2009, **5**, 1775-1785.
13. K. Koren, S. M. Borisov, R. Saf and I. Klimant, *European Journal of Inorganic chemistry*, 2011, **2011**, 1531-1534.
14. C. von Bultzingslowen, A. K. McEvoy, C. McDonagh, B. D. MacCraith, I. Klimant, C. Krause and O. S. Wolfbeis, *The Analyst*, 2002, **127**, 1478-1483.
15. M. Kameda, H. Seki, T. Makoshi, Y. Amao and K. Nakakita, *Sensors and Actuators B: Chemical*, 2012, **171-172**, 343-349.
16. Y. Tian, B. R. Shumway and D. R. Meldrum, *Chemistry of Materials*, 2010, **22**, 2069-2078.
17. A. V. Volkov, A. A. Tunyan, M. A. Moskvina, A. L. Volynskii, A. I. Dement'ev and N. F. Bakeev, *Polymer Science Series A*, 2009, **51**, 563-570.
18. D. B. Papkovsky, A. N. Ovchinnikov, V. I. Ogurtsov, G. V. Ponomarev and T. Korpela, *Sensors and Actuators B: Chemical*, 1998, **51**, 137-145.
19. D. B. Papkovsky, T. C. O'Riordan and G. G. Guilbault, *Analytical chemistry*, 1999, **71**, 1568-1573.
20. A. Mills, *Chemical Society Reviews*, 2005, **34**, 1003-1011.
21. T. C. M. Chung, *Macromolecules*, 2013, **46**, 6671-6698.
22. R. N. Gillanders, O. V. Arzhakova, A. Hempel, A. Dolgova, J. P. Kerry, L. M. Yarysheva, N. F. Bakeev, A. L. Volynskii and D. B. Papkovsky, *Analytical chemistry*, 2009, **82**, 466-468.
23. A. Mills and A. Graham, *The Analyst*, 2013, **138**, 6488-6493.
24. Q. Xu, J. Yang, J. Dai, Y. Yang, X. Chen and Y. Wang, *Journal of Membrane Science*, 2013, **448**, 215-222.
25. H. Boukehili and P. Nguyen-Tri, *Journal of Reinforced Plastics and Composites*, 2012, **31**, 1638-1651.
26. Z.P. Zhao, M.S. Li, N. Li, M.X. Wang and Y. Zhang, *Journal of Membrane Science*, 2013, **440**, 9-19.
27. T.H. Cho, M. Tanaka, H. Ohnishi, Y. Kondo, M. Yoshikazu, T. Nakamura and T. Sakai, *Journal of Power Sources*, 2010, **195**, 4272-4277.
28. R. van Reis and A. Zydney, *Journal of Membrane Science*, 2007, **297**, 16-50.
29. H.Y. Guan, F. Lian, Y. Ren, Y. Wen, X.R. Pan and J.I. Sun, *Int J Miner Metall Mater*, 2013, **20**, 598-603.
30. C. Wu, B. Bull, K. Christensen and J. McNeill, *Angewandte Chemie International Edition*, 2009, **48**, 2741-2745.
31. F. N. Limited, 2006.
32. J. H. Lee, I. J. Gomez, V. B. Sitterle and J. C. Meredith, *Journal of colloid and interface science*, 2011, **363**, 137-144.
33. Z. Ding, R. Bao, B. Zhao, J. Yan, Z. Liu and M. Yang, *Journal of Applied Polymer Science*, 2013, **130**, 1659-1666.
34. G. Di Marco, M. Lanza, M. Pieruccini and S. Campagna, *Advanced Materials*, 1996, **8**, 576-580.
35. P. Jin, Z. Guo, J. Chu, J. Tan, S. Zhang and W. Zhu, *Industrial & Engineering Chemistry Research*, 2013, **52**, 3980-3987.
36. C. Baleizão, S. Nagl, M. Schäferling, M. r. N. Berberan-Santos and O. S. Wolfbeis, *Analytical chemistry*, 2008, **80**, 6449-6457.
37. G. Liebsch, I. Klimant and O. S. Wolfbeis, *Advanced Materials*, 1999, **11**, 1296-1299.
38. K. Eaton and P. Douglas, *Sensors and Actuators B: Chemical*, 2002, **82**, 94-104.

39. K. A. Kneas, J. N. Demas, B. A. DeGraff and A. Periasamy, *Microscopy and Microanalysis*, 2000, **6**, 551-561.